

# On C–C Coupling by Carbene-Stabilized Palladium Catalysts: A Density Functional Study of the Heck Reaction

Katrin Albert, Philip Gisdakis, and Notker Rösch\*

Lehrstuhl für Theoretische Chemie, Technische Universität München,  
D-85747 Garching, Germany

Received October 21, 1997

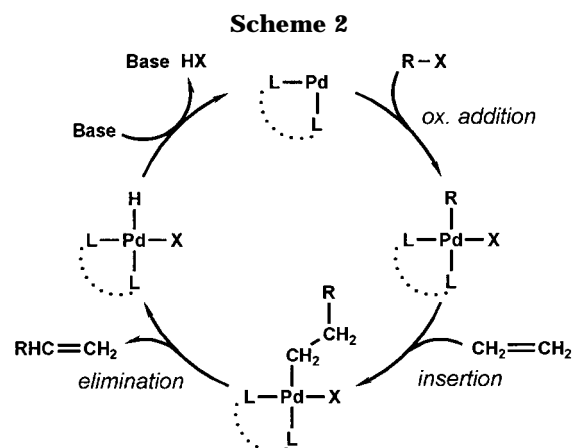
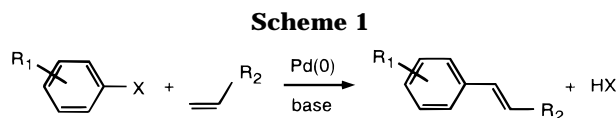
The mechanism of the Heck reaction has been computationally studied for a carbene-stabilized palladium catalyst employing a density functional method with a gradient-corrected exchange-correlation functional. The crucial steps of the reaction, insertion of the olefin into the Pd–aryl bond and  $\beta$ -hydride elimination, have been investigated for a Pd catalyst ligated by two diaminocarbene ligands; these ligands have been chosen to model 1,3-dimethylimidazol-2-ylidene ligands which have been employed in experimental work. The reaction involves the cleavage of a Pd–halide bond and thus proceeds via positively charged complexes. For the insertion, the effect of a counterion has also been investigated; its presence does not alter the reaction mechanism since its influence on the reaction energies is small. The insertion step has also been studied for a newly proposed bidentate ligand which coordinates to the Pd center via one carbene as well as one phosphine group. In this system, a Pd–P bond is broken, leading to neutral intermediates. For both ligand systems, the calculated barriers to insertion are in the range 8.3–11.5 kcal/mol; the barrier to  $\beta$ -hydride elimination is calculated as 9.0 kcal/mol.

## I. Introduction

The palladium-catalyzed C–C-coupling reaction of an aryl or alkenyl halide with an olefin shown in Scheme 1 is known as the Heck reaction.<sup>1,2</sup> The catalyst in the standard system is a palladium(0) species which is stabilized by two phosphine ligands, usually triarylphosphines. The reactivity of the aryl halide component decreases in the order  $X = I > Br > Cl$ , and electron-withdrawing substituents  $R_1$  are required for the latter to react.<sup>3</sup> A drawback of the classical Heck reaction is that it is confined to temperatures below 120 °C, where the preparatively most interesting aryl chlorides do not react.<sup>4</sup> Above this temperature a deactivation of the catalyst due to P–C bond rupture is observed.<sup>4</sup>

A schematic representation of the catalytic cycle of the Heck reaction as discussed in the literature is given in Scheme 2.<sup>2</sup> The catalyst is a 14-electron  $Pd^0L_2$  species, where L is usually a monodentate or bidentate phosphine. The first step consists of the oxidative addition of an aryl halide  $R_1X$  to the catalyst, followed by the insertion of the olefin into the Pd–aryl bond. The product is extruded via a  $\beta$ -hydride elimination, and the catalyst is regenerated by a base-assisted HX elimination.

The oxidative addition of an aryl halide to a complex  $ML_2$  ( $M = Pd, Pt$ ) is a well-known organic reaction and has been the subject of many experimental investiga-



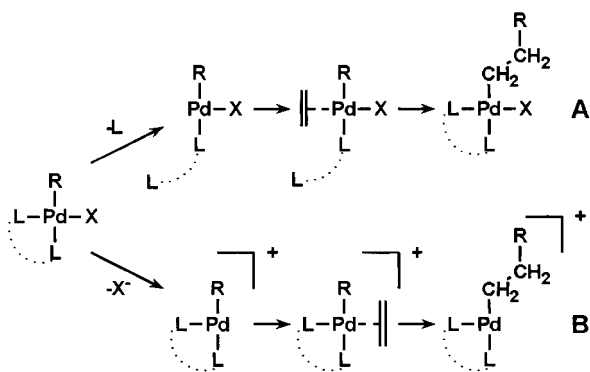
tions.<sup>5–12</sup> If  $L_2$  is a bidentate ligand, the cis product is formed,<sup>9,12</sup> whereas otherwise usually the trans product

\* Corresponding author.

(1) de Meijere, A.; Meyer, F. E. *Angew. Chem.* **1994**, *106*, 2473.  
(2) Cabri, W.; Candiani, I. *Acc. Chem. Res.* **1995**, *28*, 2.  
(3) Heck, R. F. *Acc. Chem. Res.* **1979**, *12*, 146.  
(4) Herrmann, W. A.; Brossmer, C.; Öfele, K.; Beller, M.; Fischer, H. *J. Organomet. Chem.* **1995**, *491*, C1.

(5) Fitton, P.; McKeon, J. E. *J. Chem. Soc., Chem. Commun.* **1968**, 4.  
(6) Fitton, P.; Johnson, M. P.; McKeon, J. E. *J. Chem. Soc., Chem. Commun.* **1968**, 6.  
(7) Fitton, P.; Rick, E. A. *J. Organomet. Chem.* **1971**, *28*, 287.  
(8) DiBugno, C.; Pasquali, M.; Leoni, P.; Sabatino, P.; Braga, D. *Inorg. Chem.* **1989**, *28*, 1390.  
(9) Herrmann, W. A.; Brossmer, C.; Priermeier, T.; Öfele, K. *J. Organomet. Chem.* **1994**, *481*, 97.  
(10) Urata, H.; Tanaka, M.; Fuchikami, T. *Chem. Lett.* **1987**, 751.  
(11) Amatore, C.; Azzabi, M.; Jutand, A. *J. Am. Chem. Soc.* **1991**, *113*, 8375.  
(12) Portnoy, M.; Milstein, D. *Organometallics* **1993**, *12*, 1665.

Scheme 3



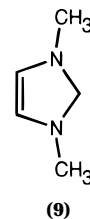
is obtained.<sup>5-9</sup> The reaction rate depends on the substituents of the phenyl ring; electron-withdrawing groups like CHO and good leaving groups X (I > Br > Cl) facilitate the addition.<sup>1,7</sup>

Two different reaction pathways have been proposed for the insertion process<sup>2</sup> (Scheme 3): path A involves the dissociation of a ligand-Pd bond leading to neutral species; path B implicates the loss of an anionic ligand and the formation of cationic intermediates. In the standard Heck reaction involving aryl halides, the complex formed after the oxidative addition contains a rather weak Pd-PR<sub>3</sub> bond (or Pd-solvent bond if phosphine ligands are not present) and a stronger Pd-X (X = I, Br, Cl) bond. Thus, the neutral ligand dissociates before coordination of the olefin (path A). A new situation arises when aryl triflates instead of aryl halides are used in the reaction due to the labile Pd-OTf (OTf = trifluoromethanesulfonate) bond present in the oxidative addition complex. It has been proposed recently<sup>3,14</sup> that in this case the insertion is accompanied by the dissociation of the counterion (path B). Along both reaction pathways, the insertion can take place only if the olefin coordinates cis to the aryl ligand.<sup>15</sup>

The product is formed via intramolecular  $\beta$ -hydride elimination; for this to occur the migrating hydride and the vacant coordination site have to be situated syn to each other.<sup>1</sup> Thus, an internal rotation of the insertion product around the C-C bond is required before the elimination step.

Novel developments concerning other types of ligands L open a wide field of applications for the Heck reaction. For example, a very high catalytic activity is observed for palladacycles;<sup>16</sup> recently, experiments on palladium complexes which are stabilized by N-heterocyclic carbenes like **9** were reported, whose advantage lies in their unusual stability against heat, oxygen and moisture.<sup>17</sup>

In the present work, we investigated the Heck reaction involving this new type of carbene-stabilized palladium catalyst using density functional calculations in order to address the following questions: (i) Does this reaction follow one of the pathways proposed in the literature? (ii) What are the energetics of the reaction?



In the calculations, the crucial steps of the reaction (insertion,  $\beta$ -hydride elimination) have been studied for a catalyst PdL<sub>2</sub> where L = diaminocarbene is chosen as a model for the experimentally used ligand 1,3-dimethylimidazol-2-ylidene shown as **9**. The olefin component is modeled by ethylene and the aryl halide by bromobenzene. We present a reaction mechanism which resembles that of the ethylene polymerization reaction catalyzed by Ni(II)- or Pd(II)-diimine complexes; recently, this reaction has been thoroughly studied with density functional methods.<sup>18-22</sup>

Furthermore, we have studied the insertion of ethylene for a bidentate ligand in which a carbene moiety is connected via a CH<sub>2</sub> bridge to a phosphine group. In this system, the aryl halide is modeled by chlorobenzene.

## II. Computational Details

All density functional calculations have been performed with the program Gaussian 94.<sup>23</sup> An exchange-correlation functional with density gradient corrections as proposed by Becke<sup>24</sup> and Perdew<sup>25,26</sup> has been employed throughout. The geometry optimizations have been carried out using standard double- $\zeta$  basis sets (LANL2DZ) and effective core potentials (ECPs) for the heavy elements.<sup>27,28</sup> An all-electron description at the same double- $\zeta$  level was used for elements of the first row.<sup>29</sup> For Pd, relativistic effects are accounted for by the ECPs; the 4s and 4p orbitals of Pd were treated as part of the valence shell (small core ECP). The energies of the stationary points were recalculated with the LANL2DZ basis set on Pd and a 6-311G\*\* basis set<sup>30</sup> on all other atoms in order to obtain more accurate energies. Partial charges were derived from a Mulliken

(18) Margl, P.; Ziegler, T. *J. Am. Chem. Soc.* **1996**, *118*, 7337.

(19) Svensson, M.; Matsubara, T.; Morokuma, K. *Organometallics* **1996**, *15*, 5568.

(20) Deng, L.; Margl, P.; Ziegler, T. *J. Am. Chem. Soc.* **1997**, *119*, 1094.

(21) Musaev, D. G.; Froese, R. D. J.; Svensson, M.; Morokuma, K. *J. Am. Chem. Soc.* **1997**, *119*, 367.

(22) Musaev, D. G.; Svensson, M.; Morokuma, K.; Strömberg, S.; Zetterberg, K.; Siegbahn, P. E. M. *Organometallics* **1997**, *16*, 1933.

(23) Gaussian 94, Revision D.4: M. J. Frisch, G. W. Trucks, H. B. Schlegel, P. M. W. Gill, B. G. Johnson, M. A. Robb, J. R. Cheeseman, T. Keith, G. A. Petersson, J. A. Montgomery, K. Raghavachari, M. A. Al-Laham, V. G. Zakrzewski, J. V. Ortiz, J. B. Foresman, J. Cioslowski, B. B. Stefanov, A. Nanayakkara, M. Challacombe, C. Y. Peng, P. Y. Ayala, W. Chen, M. W. Wong, J. L. Andres, E. S. Replogle, R. Gomperts, R. L. Martin, D. J. Fox, J. S. Binkley, D. J. Defrees, J. Baker, J. P. Stewart, M. Head-Gordon, C. Gonzalez, J. A. Pople, Gaussian, Inc., Pittsburgh, PA, 1995.

(24) Becke, A. D. *Phys. Rev. A* **1988**, *38*, 3098.

(25) Perdew, J. P. *Phys. Rev. B* **1986**, *33*, 8822.

(26) Perdew, J. P. *Phys. Rev. B* **1986**, *34*, 7406.

(27) Hay, P. J.; Wadt, W. R. *J. Chem. Phys.* **1985**, *82*, 299.

(28) Wadt, W. R.; Hay, P. J. *J. Chem. Phys.* **1985**, *82*, 284.

(29) Dunning, T. H.; Hay, P. J. In *Modern Theoretical Chemistry*; Schaefer, H. F., III, Ed.; Plenum Press: New York and London, 1976; Vol. 3, p 1.

(30) Krishnan, R.; Binkley, J. S.; Seeger, R.; Pople, J. A. *J. Chem. Phys.* **1980**, *72*, 650.

(13) Cabri, W.; Candiani, I.; DeBernadinis, S.; Francalanci, F.; Penco, S.; Santi, R. *J. Org. Chem.* **1991**, *56*, 5796.

(14) Ozawa, F.; Kubo, A.; Hayashi, T. *J. Am. Chem. Soc.* **1991**, *113*, 1417.

(15) Thorn, D. L.; Hoffmann, R. *J. Am. Chem. Soc.* **1978**, *100*, 2079.

(16) Herrmann, W. A.; Brossmer, C.; Öfele, K.; Reisinger, C.-P.; Priermeier, T.; Beller, M.; Fischer, H. *Angew. Chem.* **1995**, *107*, 1989.

(17) Herrmann, W. A.; Elison, M.; Fischer, J.; Köcher, C.; Artus, G. R. *J. Angew. Chem.* **1995**, *107*, 2602.

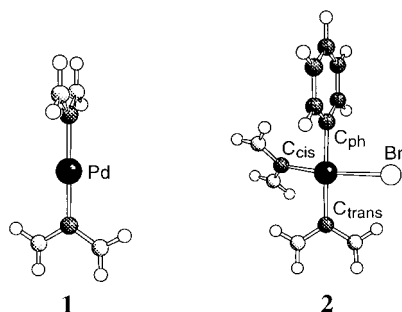


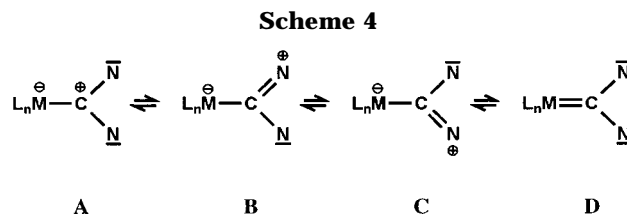
**Figure 1.** Optimized geometries of the free catalyst **1** and the cis product **2** of the oxidative addition of bromobenzene.

population analysis. Most molecules were optimized without symmetry constraints; exceptions are chloro- and bromobenzene ( $C_{2v}$ ) and bis(diamino)carbenepalladium(0) **1** ( $D_{2d}$ ) as well as 1-methylenephosphine-imidazol-2-ylidenepalladium(0) **1'**, chloro(1-methylenephosphine-imidazol-2-ylidene)phenylpalladium(II) **2'**, and **TS(i)c** ( $C_s$ ), the transition state for the ethylene insertion (for details see section III, A, B, and E). Transition states have been located by employing the reaction coordinate method followed by a transition-state search based on the Berny algorithm as implemented in Gaussian 94.<sup>31</sup> One exception is the transition state **TS(e)c** of the  $\beta$ -hydride elimination in which the distance  $C_{\beta}$ -H has been varied as the reaction coordinate. For a value of 1.71 Å a maximum of the total energy was found; the gradient on this coordinate is  $-4 \times 10^{-5}$  au, all other gradients being smaller. All transition states were checked to have one negative eigenvalue of the Hessian.

Before presenting the results, we would like to briefly comment on the basis sets used. As already mentioned, we optimized the geometries using effective core potentials (LANL2DZ basis) and recalculated the energy using a larger basis set (6-311G\*\*) on all atoms except for Pd. We illustrate the quality of this computational strategy by comparing the ligand-binding energy of Pd-C(NH<sub>2</sub>)<sub>2</sub> at three levels of computation. For the procedures LANL2DZ//LANL2DZ, 6-311G\*\*//LANL2DZ, and 6-311G\*\*//6-311G\*\* on the ligand (treating Pd always at the LANL2DZ/ECP level) the binding energy values are 62.3, 58.8, and 58.5 kcal/mol, respectively. Thus, while enlarging the ligand basis set changes the binding energy by about 6%, the geometry optimization in the larger basis has an influence of less than 1%. Thus, we conclude that for the present purpose, that is, the calculation of a reaction path, the 6-311G\*\*//LANL2DZ strategy (for the ligands) will provide sufficiently accurate results.

### III. Results and Discussion

**A. The Catalyst.** The Pd(0) catalyst employed by Herrmann et al.<sup>17</sup> bears two 1,3-dimethylimidazol-2-ylidene ligands. In the calculations, this carbene has been modeled by diaminocarbene. The optimized geometry of bis(diaminocarbene)palladium(0) **1** is displayed in Figure 1. The complex is linearly coordinated, and the planes of the carbene ligands are perpendicular to each other. The interaction of a transition-metal



center with a carbene ligand is well-understood.<sup>32,33</sup> The metal-carbene bonding can be represented by the resonance structures shown in Scheme 4. **A–C** illustrate the bonding situation in heteroatom-substituted (Fischer) carbenes, whereas **D** applies to alkyl-substituted (Schrock) carbenes.<sup>32</sup> The importance of the resonance structures **B** and **C** in bis(diaminocarbene)-palladium(0) is demonstrated by the calculated length of the C–N bond (1.38 Å), which is shorter than a typical  $sp^2$ -C–N bond, 1.45 Å.<sup>34</sup> Electronic charge is donated from the ligands to the metal,  $q(\text{Pd}) = -0.32$  au. The calculated Pd–carbene bond length, 2.02 Å, lies within the range of experimental values reported for a Pd–C single bond (1.99–2.05 Å<sup>17</sup>). The Pd–C bond exhibits only rather minor double-bond character as reflected by the low barrier to rotation of one ligand around this bond which is calculated as 1.8 kcal/mol.

The calculated total binding energy of both carbene ligands to the Pd center is 105.3 kcal/mol. The quality of our model carbene can be demonstrated by the similarity of its binding energy and charge distribution to that of the experimentally used ligand 1,3-dimethylimidazol-2-ylidene. Two of these latter ligands exhibit a binding energy of 106.9 kcal/mol, a value which is very close to that calculated for the model system. The charge on Pd is slightly lower in the “real” system,  $q(\text{Pd}) = -0.29$  au instead of  $-0.32$  au in the model system. The Pd–carbene bond distance is the same in both complexes (2.02 Å). Although the experimentally used carbene ligand (**9**) is sterically more demanding than our model diaminocarbene, the calculated barrier to rotation of a carbene ligand around the Pd–C bond is exactly the same in both systems, 1.8 kcal/mol. Due to the strained five-membered ring in 1,3-dimethylimidazol-2-ylidene, the angle N–C–N, 102.4°, is significantly smaller in this compound than the one in our model carbene, 113.9°. To evaluate our model, we reoptimized the catalyst **1** with the angle N–C–N fixed to 102.4°. The calculated binding energy of the diaminocarbene ligands decreases significantly for this molecule, to 94.0 kcal/mol. The Pd–carbene bond distance amounts to 2.00 Å and is thus shorter than that in the unrestricted bis(diaminocarbene)palladium(0) by 0.02 Å. Thus, fixing the N–C–N angle does not lead to an improvement of the model. Compared to two phosphine ligands, the Pd–carbene binding energy is calculated to be noticeably stronger, by about 25%. The binding energy of the experimentally used triphenylphosphine can be modeled with sufficient accuracy by trimethylphosphine.<sup>35</sup> The binding energy of two trimethylphosphine ligands to Pd is calculated to be 83.9 kcal/mol, to be compared to the value of about 105.3 kcal/mol for two carbene ligands.

(32) Schubert, U. In *Transition Metal Carbene Complexes*; VCH: Weinheim, 1983; p 73.

(33) Siegbahn, P. E. M. *Chem. Phys. Lett.* **1993**, *201*, 15.

(34) Elschenbroich, C.; Salzer, A. *Organometallics*; B. G. Teubner: Stuttgart, 1990.

(35) Häberlen, O. D.; Rösch, N. *J. Phys. Chem.* **1993**, *97*, 4970.

(31) Schlegel, H. B. *J. Comput. Chem.* **1982**, *3*, 214.

**Table 1.** Calculated Geometrical Parameters and Partial Charges  $q$  of the Intermediates and Transition State of the Insertion of Ethylene into the Pd–Phenyl Bond for the Cationic (c) and Neutral (n) Pathways as Well as Energy Differences  $\Delta E$  between Successive Stationary Points along the Path<sup>a</sup>

	3c + C <sub>2</sub> H <sub>4</sub>	4c	5c	TS(i)c	6c	2 + C <sub>2</sub> H <sub>4</sub>	4n	5n	TS(i)n	6n
Pd–C <sub>trans</sub>	2.13	2.13	2.11	2.05	2.00	2.13	2.12	2.10	2.04	1.99
Pd–C <sub>cis</sub>	1.99	2.04	2.03	2.08	2.12	2.01	2.04	2.03	2.07	2.11
Pd–C <sub>ph</sub>	2.02	2.07	2.11	2.18	2.48	2.06	2.07	2.10	2.18	2.48
Pd–C <sub>α</sub>		2.34	2.33	2.16	2.11		2.31	2.31	2.15	2.11
Pd–C <sub>β</sub>		2.34	2.34	2.43	2.79		2.32	2.31	2.40	2.81
C <sub>β</sub> –C <sub>ph</sub>		3.11	2.71	2.11	1.54		3.12	2.72	2.05	1.54
C <sub>α</sub> –C <sub>β</sub>	1.36 <sup>b</sup>	1.39	1.40	1.44	1.55	1.36 <sup>b</sup>	1.40	1.40	1.45	1.55
Pd–Br						2.60	3.65	3.74	3.63	3.76
$q(\text{Pd})$	0.34	0.04	0.05	0.09	0.08	0.19	0.05	0.05	0.08	–0.06
$q(\text{carbene}_{\text{trans}})$	0.30	0.38	0.39	0.39	0.43	0.22	0.28	0.29	0.30	0.33
$q(\text{carbene}_{\text{cis}})$	0.46	0.39	0.39	0.36	0.33	0.26	0.29	0.30	0.26	0.24
$q(\text{phenyl})$	–0.10	–0.14	–0.13	–0.11	0.16 <sup>c</sup>	–0.28	–0.24	–0.22	–0.19	0.04 <sup>c</sup>
$q(\text{ethylene})$	0.00	0.33	0.29	0.26		0.00	0.27	0.24	0.21	
$q(\text{Br})$						–0.39	–0.65	–0.65	–0.66	–0.67
$\Delta E$		–19.5	+0.1	+8.2	–23.6		–5.3	+0.5	+11.0	–21.4

<sup>a</sup> Bond lengths in Å, charges in au, energies in kcal/mol. <sup>b</sup> Value in free ethylene. <sup>c</sup> Compounded value for the phenyl and ethylene moieties.

**B. Oxidative Addition.** The cis product **2** of the oxidative addition which is obtained after addition of bromobenzene to **1** is displayed in Figure 1. Selected bond lengths and atomic charges are given in Table 1. While the formal oxidation state of the metal in this complex is +II, the Pd center bears only a small positive charge, 0.19 au. There are two different Pd–carbene bond lengths: the one cis to the phenyl ring is slightly shorter (by 0.01 Å) than in the free catalyst (2.02 Å), and the one in the trans position is 0.11 Å longer (Table 1). This can be rationalized by the trans influence, that is, the capability of a ligand to weaken a bond trans to it. C<sub>6</sub>H<sub>5</sub><sup>–</sup> is known to exhibit a stronger trans influence than Br<sup>–</sup>, thus leading to a larger Pd–carbene<sub>trans</sub> bond distance.<sup>36</sup> The C–N bond distances in **2** are slightly smaller than in **1**, ranging from 1.35 to 1.38 Å; this finding indicates a larger contribution of the resonance structures **B** and **C**. With a dihedral angle  $\angle(\text{Br–Pd–C}_{\text{trans}}\text{–N}) = 10^\circ$ , the trans carbene ligand lies almost in the coordination plane of the Pd center while the cis carbene ligand has a more upright conformation,  $\angle(\text{C}_{\text{ph}}\text{–Pd–C}_{\text{cis}}\text{–N}) = 36^\circ$ . In the trans product of the oxidative addition (not shown), both carbene moieties lie in the PdL<sub>4</sub> coordination plane. Thus, it seems that the orientation of the carbene ligands relative to the PdL<sub>4</sub> plane is determined by electrostatic attraction between the carbene substituents and the Br center. This geometrical feature may, at least in part, be due to the model ligand chosen. The oxidative addition is an exothermic process; the calculated energy for the reaction **1** + bromobenzene → **2** is –34.1 kcal/mol.

**C. Insertion.** To allow for a coordination of the olefin to the Pd center, a vacant coordination site is required. The Pd–carbene bond is stronger than the Pd–phosphine bond present in the product of the oxidative addition to a Pd–diphosphine complex. In experiment, no free carbene could be observed.<sup>37</sup> Thus, in the present calculations, both carbene ligands have been kept coordinated to the Pd center along the reaction pathways investigated, as in path B of Scheme 3 where dissociation of Br<sup>–</sup> is assumed. Besides this

cationic path (in the following denoted by **c**), also a neutral variant (denoted by **n**) has been studied where the halide center is kept in the vicinity of the catalyst. The “neutral” pathway B’ starts from the product of the oxidative addition **2** and leads to complexes with a total charge of 0 (**4n**–**6n**, not shown). On the other hand, the proper “cationic” path B (Scheme 3) starts from complex **3c**, which is obtained after removal of the bromine anion from **2** (Figure 2), and involves singly positively charged species (**4c**–**6c**).

It is instructive to compare the two pathways B and B’ because they allow for a detailed understanding of the role of a counterion during the insertion process. Interesting questions in this context are as follows: (i) Is the mechanism of the insertion altered by the presence of a counterion? (ii) Is the energy barrier significantly affected? (iii) Does the geometry of the stationary points change? Of course, a single atom like Br<sup>–</sup> cannot replace a proper treatment of the solvent effects; nevertheless one may expect that a comparison of the cationic and neutral pathways provides indications as to whether calculations of isolated complexes represent too strong a simplification.

The optimized geometries of the cationic species involved in the insertion process are shown in Figure 2. We find that the mechanism of the insertion is independent of the presence of Br<sup>–</sup>, that is, the stationary points resemble each other in both pathways. In all neutral complexes, the Br<sup>–</sup> ion is located above the PdL<sub>4</sub> coordination plane at a distance (3.63–3.76 Å) considerably larger than the sum of the corresponding covalent radii (2.51 Å<sup>38</sup>). The position of the bromine ion is exemplified in Figure 3 for the transition state of insertion **TS(i)**. The geometry of the complex PdL<sub>4</sub> is not much affected by the presence of the Br<sup>–</sup> counterion as can be deduced by detailed inspection of Table 1. Differences in relevant bond distances between analogous complexes of paths **c** and **n** are at most 0.03 Å; one exception is the transition state of insertion **TS(i)** (see below). Thus we shall focus our discussion on the cationic pathway proper and compare to the corresponding neutral species whenever there are noteworthy

(36) Greenwood, N. N.; Earnshaw, A. *Chemistry of the Elements*; Plenum Press: Oxford, 1984; p 1352.

(37) Fischer, J. Dissertation, Technische Universität München, 1996.

(38) Greenwood, N. N.; Earnshaw, A. *Chemistry of the Elements*; Plenum Press: Oxford, 1984; pp 934, 1333.

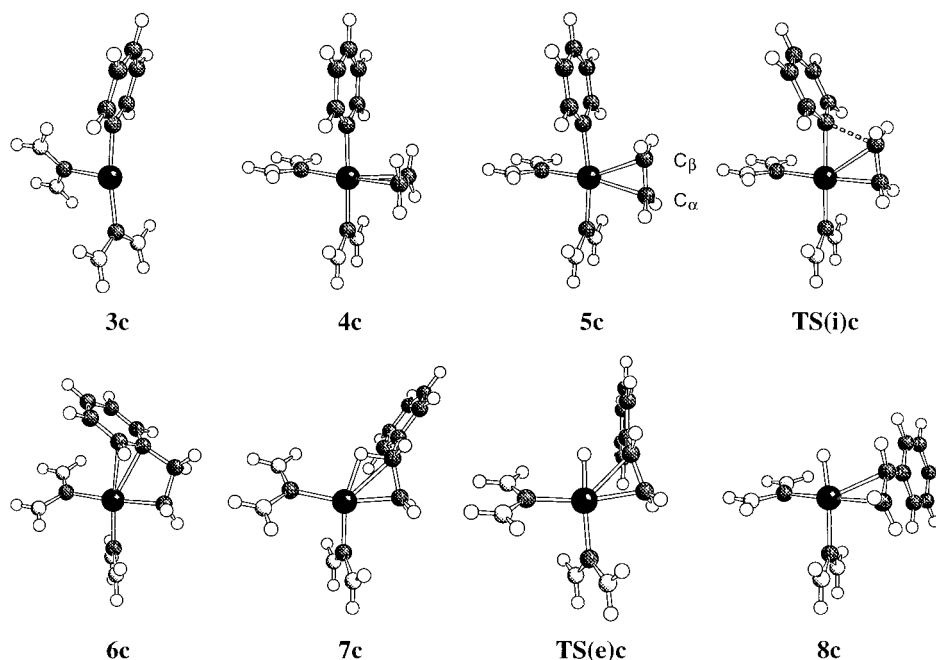


**Figure 2.** Optimized geometries of the stationary points of the ethylene insertion **3c** to **6c** and of the  $\beta$ -H elimination process **7c** to **8c** (cationic pathway).

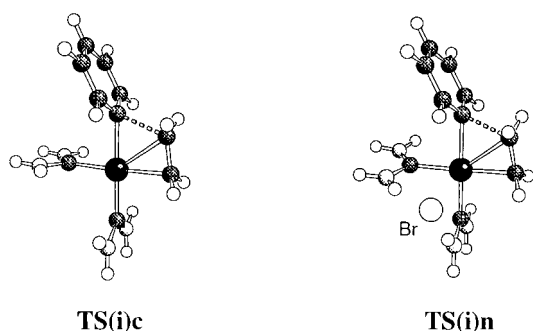


**Figure 3.** Optimized geometries of the transition states of insertion for the cationic pathway, **TS(i)c**, and the neutral pathway, **TS(i)n**.

differences. Important bond lengths are given in Table 1 together with the partial charges on the central atom and the ligands, and the calculated energy differences between successive stationary points. The energetics of both processes are compared in Figure 4. It should be noted that the starting points for the cationic and the neutral pathway are chosen differently, normalized at 0 kcal/mol; in the former case it is the three-coordinated complex **3c**, in the latter case the product **2** of the oxidative addition.

**(a) Coordination of Ethylene.** Removal of Br<sup>-</sup> from **2** is a strongly endothermic process ( $\Delta E = 114.9$  kcal/mol). This energy can be regarded as artificially high since the neutral complex **2** is separated into two charged species (**3c** and Br<sup>-</sup>), which in our calculations are not subject to a stabilization by the polar solvent. An estimate of the solvation energy of the ions using the Born model<sup>39</sup> gives a stabilization of approximately 110 kcal/mol, supporting the feasibility of the cationic pathway. Removal of the bromine ion entails a decrease of the angle C<sub>ph</sub>-Pd-C<sub>trans</sub> from 174.8° to 169.4° in **3c** and a rotation of the trans carbene ligand out of the Pd

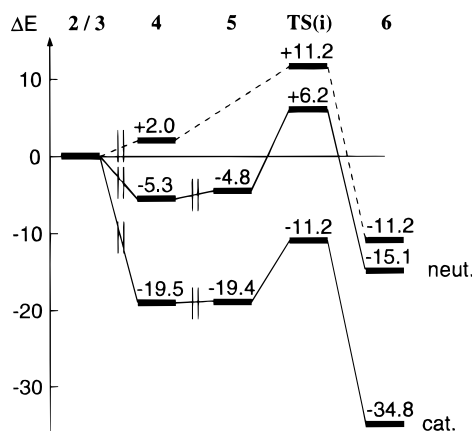


**Figure 4.** Insertion of ethylene into the Pd-phenyl bond. Energy differences  $\Delta E$  (in kcal/mol) relative to the educts, which are ethylene as well as **3c** for the cationic system, **2** for the neutral pathway of the dicarbene system (solid lines), and **2'** for the carbene-phosphine system (broken lines), all normalized at 0 kcal/mol.

coordination plane since the favorable electrostatic interaction with the Br center is no longer present. The first step of the insertion process involves the coordination of the ethylene to complex **3c**, yielding **4c** (Figure 2). The olefin occupies the coordination site of the Br center in **2**. As expected for a d<sup>8</sup> ML<sub>3</sub> complex, ethylene has an upright conformation.<sup>40</sup> This orientation is also found in the prototypical transition-metal-olefin complex, Zeise's salt K[Pt( $\eta^2$ -C<sub>2</sub>H<sub>4</sub>)Cl<sub>3</sub>].<sup>41</sup> However, the main factor which determines the orientation of the olefin is believed to be steric and not electronic,<sup>40</sup> and indeed the sterically unhindered complex [Pt( $\eta^3$ -CH<sub>2</sub>-CMeCH<sub>2</sub>)(PPh<sub>3</sub>)(CH<sub>2</sub>=CHPh)]<sup>+</sup> has been characterized in which the olefin is lying in the coordination plane of

(40) Albright, T. A.; Hoffmann, R.; Thibault, J. C.; Thorn, D. L. *J. Am. Chem. Soc.* **1979**, *101*, 3801.

(41) Love, R. A.; Koetzle, T. F.; Williams, G. J. B.; Andrews, L. C.; Bau, R. *Inorg. Chem.* **1975**, *14*, 2653.

(39) Born, M. *Z. Phys.* **1920**, *1*, 45.

the metal center.<sup>42</sup> Rotation of ethylene leads to complex **5c**, which was confirmed to be a local minimum; it is only 0.1 kcal/mol less stable than **4c**. The barrier to rotation has not been determined, but is expected to be very low.<sup>19,22</sup>

In general, the interaction of an olefin with a metal center can be described in terms of  $\sigma$  donation and  $\pi$  back-donation (Dewar–Chatt–Duncanson model<sup>43,44</sup>). Electron charge density is transferred from the filled ethylene  $\pi$  orbital to an empty metal d orbital and back from a filled metal d orbital to the ethylene  $\pi^*$  orbital. Both interaction channels lead to an elongation of the olefin C=C bond and a loss of planarity at the carbon atoms. Thus a comparison of the geometry of the coordinated ethylene to that of the free molecule should provide an indication for the strength of the metal–olefin interaction. The  $C_\alpha$ – $C_\beta$  bond distance in **4c** is slightly enlarged with respect to free ethylene (+0.03 Å); the  $CH_2$  plane deviates from planarity by only 10°. In the neutral system, the Pd– $C_{\alpha\beta}$  distance is somewhat shorter and the  $C_\alpha$ – $C_\beta$  distance is slightly longer than in the cationic complex (Table 1). Nevertheless, the interaction energy  $\Delta E$  is smaller in the presence of the bromide by 14.2 kcal/mol (see Table 1 and Figure 4). This difference can be rationalized by the fact that the three-coordinated complex **3c** is a coordinatively unsaturated species and the addition of a fourth ligand is clearly an exothermic process whereas in the neutral case  $\Delta E$  comprises additionally the energy needed to break the Pd–Br bond.

As in the product **2** of the oxidative addition, two different Pd–carbene bond lengths are found. Although usually the ethylene ligand is believed to have a stronger trans influence,<sup>36</sup> the Pd– $C_{trans}$  bond trans to the phenyl ring is longer by 0.09 Å.

**(b) The Insertion Step.** Rotation of the ethylene ligand initiates the insertion into the Pd– $C_6H_5$  bond. The Pd– $C_{ph}$  distance in **5c** is elongated by 0.04 Å in comparison to **4c**, and concomitantly, the Pd– $C_{trans}$  bond length slightly decreases. The insertion step comprises breaking the Pd– $C_{ph}$  as well as forming the Pd– $C_\alpha$  and  $C_{ph}$ – $C_\beta$  bonds. In the corresponding transition state **TS(i)c** (Figure 2), the ethylene ligand is shifted toward the phenyl ring, which in turn is bent “backward”. The  $C_\alpha$ – $C_\beta$  distance (1.44 Å) now lies between the calculated values in the free molecules ethylene and ethane (1.36 and 1.55 Å, respectively). Increased inclination of the  $CH_2$  planes (26° and 29°) also indicates the conversion to  $sp^3$ -hybridized ethylene carbon centers. In the insertion product **6c**, the free coordination site of the Pd atom is “covered” by a C–C bond of the phenyl ring with Pd–C distances of 2.48 and 2.55 Å, respectively. This interaction leads to quite an unusual geometry at the  $C_\alpha$  atom: the angle Pd– $C_\alpha$ – $C_\beta$  amounts to 98.4°, which is much smaller than the value of 109.5° expected for an  $sp^3$ -hybridized atom. A similar geometry has been found experimentally in  $[Rh(PPh_3)_3]^+$ , where the phenyl ring of one  $PPh_3$  group is tilted toward the Rh center.<sup>45</sup> The decreasing Pd– $C_6H_5$  bond strength and the forma-

**Table 2.** Calculated Geometrical Parameters and Partial Charges  $q$  of the Intermediates and Transition State of the  $\beta$ -H Elimination for the Cationic Pathway and Energy Differences  $\Delta E$  between Successive Stationary Points along the Path<sup>a</sup>

	<b>6c</b>	<b>7c</b>	<b>TS(e)c</b>	<b>8c</b>
Pd– $C_{trans}$	2.00	2.00	2.07	2.12
Pd– $C_{cis}$	2.12	2.10	2.05	2.02
Pd–H	3.35	1.91	1.65	1.61
Pd– $C_\alpha$	2.11	2.09	2.18	2.29
Pd– $C_\beta$	2.79	2.43	2.39	2.38
$C_\alpha$ – $C_\beta$	1.55	1.52	1.44	1.40
$q(Pd)$	0.08	0.05	–0.03	–0.09
$q(carbene_{trans})$	0.43	0.39	0.38	0.37
$q(carbene_{cis})$	0.33	0.32	0.36	0.40
$q(styrene)$	0.16 <sup>b</sup>	0.23 <sup>b</sup>	0.19	0.28
$q(H)$			0.10	0.04
$\Delta E$		+4.6	+4.4	–2.6

<sup>a</sup> Bond lengths in Å, charges in au, energies in kcal/mol.  
<sup>b</sup> Compounded value for the styrene and H moieties.

tion of the Pd– $C_\alpha$  bond can be monitored by the changes in the Pd–carbene bond lengths. While the Pd– $C_{trans}$  distance decreases by 0.13 Å, the Pd– $C_{cis}$  bond length is 0.08 Å longer in the insertion product **6c** as compared to **4c**. The stronger Pd– $carbene_{trans}$  interaction is reflected in a larger electronic charge transfer from this ligand while the charge on the carbene ligand in the cis position decreases (Table 1).

Inspection of the transition state **TS(i)** in the cationic and the neutral system shows that the forming  $C_{ph}$ – $C_\beta$  bond length is shorter in the latter (2.11 Å compared to 2.05 Å), that is, the presence of the counterion leads to a later transition state (see Figure 3). The angle Pd– $C_\alpha$ – $C_\beta$  is about 1° larger in **6n**, leading to a slightly larger Pd– $C_\beta$  distance. Except for the deviations mentioned, the geometrical parameters of the complexes involved in the insertion process are almost unaffected by the presence of the bromide, the differences in bond lengths being 0.03 Å or less. Interestingly, also the charge on the Pd center is very similar along the cationic and neutral pathways; the largest difference is 0.14 au in **6**. This indicates that the ligands are able to buffer the different total charges on the complex. The barrier to insertion (relative to the  $\pi$  complex **4**) amounts to +8.3 kcal/mol in the cationic system and +11.5 kcal/mol in the neutral system (Figure 4).

**D.  $\beta$ -Hydride Elimination.**  $\beta$ -Hydride elimination is initiated by a rotation of the hydrocarbon around the  $C_\alpha$ – $C_\beta$  bond leading to the  $\beta$ -agostic complex **7c** shown in Figure 2 (see also Table 2). The calculated  $C_\beta$ –H bond distance (1.20 Å) is significantly elongated in comparison to a regular C–H bond (1.11 Å calculated in ethane). This strong agostic interaction is also reflected in the unusual angle Pd– $C_\alpha$ – $C_\beta$ , which decreases from 98.4° in **6c** to 83.0° in **7c**. The  $\beta$ -agostic complex **7c** is less stable than **6c** by 4.6 kcal/mol (Figure 5), in contrast to the finding for the insertion product of ethylene into a Pd– $CH_3$  bond,<sup>22</sup> which is stabilized by 7.6 kcal/mol upon rotation around the  $C_\alpha$ – $C_\beta$  bond. This difference can be rationalized by the relative stabilization of the complex **6c** caused by the efficient interaction of the phenyl ring with the vacant coordination site of the Pd atom. In the transition state of the  $\beta$ -hydride elimination, **TS(e)c**, the  $C_\beta$ –H bond is broken

(42) Miki, K.; Kai, Y.; Kasai, N.; Kurosawa, H. *J. Am. Chem. Soc.* **1983**, *105*, 2482.

(43) Dewar, M. J. S. *Bull. Soc. Chim. Fr.* **1951**, *18*, C71.

(44) Chatt, J.; Duncanson, L. A. *J. Chem. Soc.* **1953**, 2339.

(45) Yared, Y. W.; Miles, S. L.; Bau, R.; Reed, C. A. *J. Am. Chem. Soc.* **1977**, *99*, 7076.

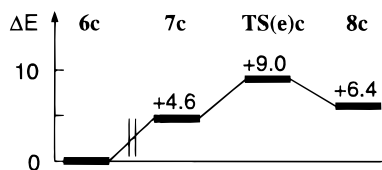


**Figure 5.**  $\beta$ -H elimination. Energy differences  $\Delta E$  (in kcal/mol) relative to **6c** (cationic pathway).

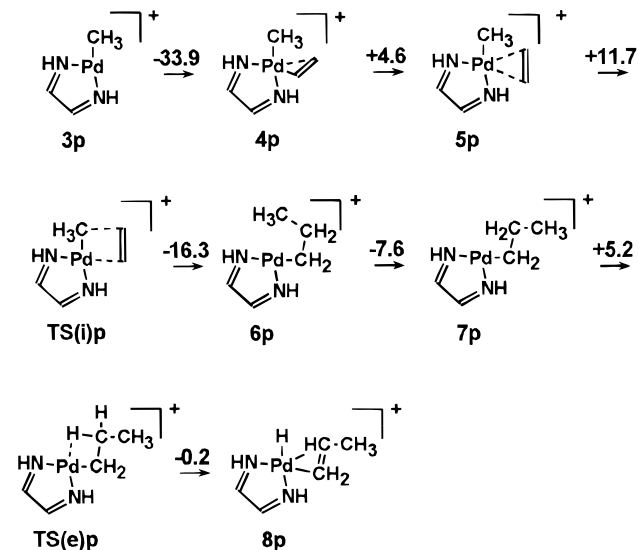


**Figure 6.** Some stationary points **3p** to **8p** of the polymerization reaction **p** of ethylene with  $\eta^2$ -(HCNH)<sub>2</sub>PdMe<sup>+</sup>.<sup>22</sup> The numbering has been chosen in accordance with the numbering in the present study. Energies are in kcal/mol.

and the Pd–H bond is formed. The Pd–C<sub>α</sub>  $\sigma$  bond is replaced by a  $\pi$  interaction with the hydrocarbon double bond. The geometrical parameters of the transition state (Table 2) are closer to the values in the product of the elimination than to those in the educt. We were not able to locate this transition state with the help of a transition-state search based on the Hessian since the potential energy surface is extremely flat in this region (see section II). This problem has already been reported for other  $\beta$ -hydride elimination processes.<sup>20,21</sup> The double bond of the styrene ligand in **8c** is not situated in the coordination plane of Pd, but is rotated out of it by 46° (dihedral angle C<sub>trans</sub>–Pd–C<sub>α</sub>–C<sub>β</sub> = 134°); the ligand is asymmetrically bonded; the Pd–C<sub>α/β</sub> bond lengths differ by 0.09 Å.

The barrier to  $\beta$ -hydride elimination (relative to the product **6c** of the insertion) amounts to +9.0 kcal/mol (Figure 5); the elimination product **8c** is 6.4 kcal/mol less stable than **6c**. The total insertion/elimination process **4c** → **8c** is exothermic by –8.9 kcal/mol.

In the following, we shall briefly compare our results to those of the above-mentioned ethylene polymerization reaction<sup>22</sup> involving a palladium–diimine catalyst. We focus on the cationic pathway since the effect of a counterion has not been considered in the other study. A schematic representation of the reaction (denoted by **p**) is given in Figure 6 together with the energy differences between successive stationary points. The geometrical features of the stationary points resemble each other in both systems. The addition of ethylene is much more exothermic (by 14.4 kcal/mol) than in the Heck system. The energy difference between the two

$\pi$  complexes **4p** and **5p** is larger, 4.6 kcal/mol, probably for steric reasons; in **5p**, two H atoms of the ligands are situated in the coordination plane of the ethylene molecule. The barrier to insertion is higher; the energy difference to the more stable  $\pi$  complex **4p** amounts to 16.3 kcal/mol in comparison to 8.3 kcal/mol in our study. The product of the insertion **6p** is isoenergetic to the  $\pi$  complex **4p** while in the Heck system there is a large energy difference between the two. This has already been rationalized by the more efficient interaction of the delocalized  $\pi$  system of the phenyl ring with the vacant coordination site at the Pd center. Thus, the  $\beta$ -agostic complex **7p** is less stable than **6p** in the Heck reaction while it is 7.6 kcal/mol lower in energy in the Pd–diimine system. The activation energies for  $\beta$ -hydride elimination are of comparable size in both systems, 5.2 and 4.4 kcal/mol, respectively. The product of the  $\beta$ -hydride elimination **8p** is almost isoenergetic to the preceding transition state **TS(e)p**. The total insertion/elimination process **4p** → **8p** is by 6.6 kcal/mol less exothermic than the process **4c** → **8c** of the dicarbene system of the Heck catalyst studied in the present work. This is probably due to the stronger C<sub>α</sub>–C<sub>ph</sub> bond in the conjugated  $\pi$  system of the styrene ligand formed during the insertion as compared to the C<sub>α</sub>–CH<sub>3</sub> single bond of the propene ligand.

**E. The Bidentate Model Ligand.** We have also investigated the mechanism of the Heck reaction for a hypothetical bidentate ligand 1-methylenephosphine-imidazol-2-ylidene **10** which is interesting for several reasons. This ligand binds to the Pd atom via a carbene moiety which has been shown to stabilize the metal center with a strong  $\sigma$  bond (Figure 7). The other end of the ligand consists of a phosphine group which forms a more labile Pd–P bond which can be reversibly broken to create a free coordination site at the Pd center. The Pd complex used in the calculations as a model for the catalyst (**1**) is shown in Figure 7. In this case the aryl halide was chosen to be chlorobenzene; the olefin component is ethylene.

The first step of the reaction consists of the oxidative addition of chlorobenzene to the catalyst **1'**. Since the bidentate ligand is asymmetric, two different products of the oxidative addition are conceivable where the phenyl ring is located either cis or trans to the phosphine ligand. Since the Pd–phosphine bond is assumed to break in the course of the reaction in order to allow for the coordination of the ethylene, it is obvious that only the cis isomer can lead to an insertion of the olefin into the Pd–phenyl bond. The optimized geometry of the cis product **2'** is displayed in Figure 7; selected bond lengths are given in Table 3. The charge distribution in this molecule is similar to that of the product **2** of the oxidative addition in the dicarbene system. Again, the carbene ligand acts as a donor of electronic charge to the Pd center to compensate the charge deficiency which is caused by the electron-withdrawing substituents Cl and phenyl. The oxidative addition is an exothermic process which releases 40.6 kcal/mol.

In the next step the Pd–phosphine bond is broken, leading to the three-coordinate Pd complex **3'** (Figure 7), which is 25.9 kcal/mol less stable than **2'**. The bidentate ligand, which is now bound only via the carbene moiety, transfers less electronic charge to the

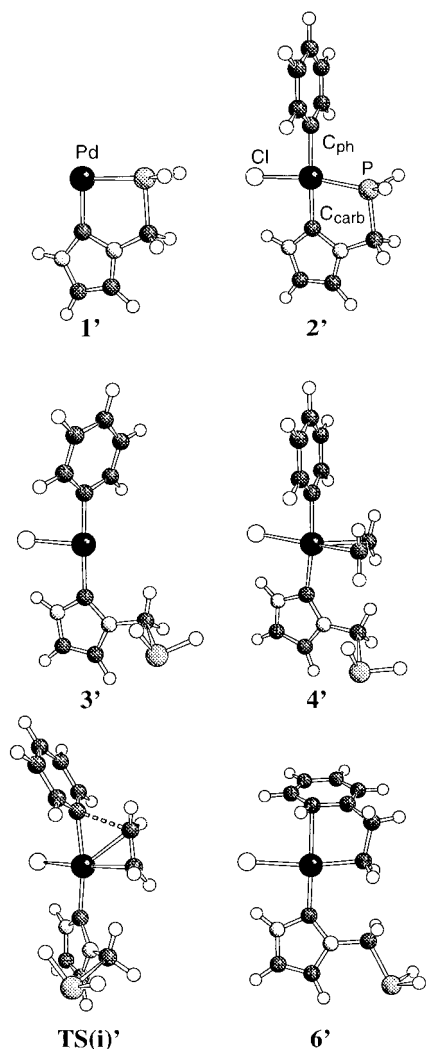


**Figure 7.** Optimized geometries of the free model catalyst 1-methylenephosphine-imidazol-2-ylidene-palladium(0) **1'** and the product **2'** of the oxidative addition of chlorobenzene as well as of the stationary points of the ethylene insertion process of the model complex **3'** to **6'**.

Pd center (0.23 au compared to 0.53 au in **2'**). Although the three-coordinate complex **3'** is neutral in contrast to the analogue **3c** of the dicarbene system, the partial charges on Pd are almost equal (+0.30 and +0.34 au, respectively). The ethylene molecule binds to the free coordination site of Pd leading to complex **4'** (Figure 7 and Table 3). As in the dicarbene system, the olefin is in an upright orientation. The energy released by the coordination of ethylene is slightly lower (by 2.0 kcal/mol) than the energy required to break the Pd–P bond (Figure 4). The Pd–C<sub>αβ</sub> distance in **4'** is 0.13 Å shorter than in the dicarbene system, and accordingly, the C<sub>α</sub>–C<sub>β</sub> bond distance is slightly longer (Tables 1 and 3). We were not able to locate a stable intermediate in which the ethylene lies in the coordination plane of the Pd center. The transition state for insertion **TS(i)'** resembles those of the dicarbene system **TS(i)c** and **TS(i)n** (cf. Figures 2 and 7). The shorter Pd–C<sub>ph</sub> and C<sub>α</sub>–C<sub>β</sub>, and the longer C<sub>β</sub>–C<sub>ph</sub> distances indicate that in **TS(i)'** this transition state is somewhat earlier than **TS(i)c** or **TS(i)n**. The barrier to insertion (+9.2 kcal/mol) lies between those for the cationic and neutral pathways in the dicarbene system. In the product **6'** of the insertion (Figure 7), the C<sub>β</sub> atom of the phenyl ring

**Table 3.** Calculated Geometrical Parameters and Partial Charges *q* of the Intermediates and Transition State of the Insertion of Ethylene into the Pd–Phenyl Bond for the Model Complex and Energy Differences  $\Delta E$  between Successive Stationary Points along the Path<sup>a</sup>

	<b>2'</b> + C <sub>2</sub> H <sub>4</sub>	<b>3'</b> + C <sub>2</sub> H <sub>4</sub>	<b>4'</b>	<b>TS(i)'</b>	<b>6'</b>
Pd–C <sub>carb</sub>	2.05	2.10	2.18	2.07	2.01
Pd–P	2.33	5.01	5.20	5.04	5.71
Pd–C <sub>ph</sub>	2.06	1.99	2.05	2.13	2.90
Pd–C <sub>α</sub>			2.21	2.14	2.09
Pd–C <sub>β</sub>			2.21	2.32	2.94
C <sub>β</sub> –C <sub>ph</sub>			2.94	2.16	1.52
C <sub>α</sub> –C <sub>β</sub>	1.36 <sup>b</sup>	1.36 <sup>b</sup>	1.41	1.44	1.55
Pd–Cl	2.43	2.41	2.45	2.50	2.56
<i>q</i> (Pd)	0.16	0.30	0.14	0.17	0.11
<i>q</i> (ligand)	0.53	0.23	0.25	0.29	0.36
<i>q</i> (phenyl)	–0.25	–0.14	–0.18	–0.11	0.09 <sup>c</sup>
<i>q</i> (ethylene)		0.00	0.21	0.14	
<i>q</i> (Cl)	–0.43	–0.39	–0.42	–0.48	–0.56
$\Delta E$		+25.9	–23.9	+9.2	–22.4

<sup>a</sup> Bond lengths in Å, charges in au, energies in kcal/mol. <sup>b</sup> Value in free ethylene. <sup>c</sup> Compounded value for the phenyl and ethylene moieties.

coordinates to the Pd center. The Pd–phenyl distance is considerably longer than in the dicarbene system, 2.90 Å compared to 2.48 Å. During the insertion process, the negative charge on the Cl atom increases (from –0.39 au in **3'** to –0.56 au in **6'**) and, simultaneously, the Pd–Cl bond distance becomes larger (from 2.41 to 2.56 Å). The energy **2'** → **6'** released with respect to the product **2'** of the oxidative addition, –11.2 kcal/mol, is by 3.9 kcal/mol smaller than that of the neutral pathway (Figure 4). Since the energetics of the insertion process for a Pd catalyst stabilized by ligand **10** is similar to that of the neutral path B' of the dicarbene system (see Figure 4), we refrained from studying  $\beta$ -H elimination for this case.

Our calculations show that the Pd catalyst with the bidentate model ligand **10** proposed by us has structural and energetical properties similar to those of the corresponding dicarbene system, making it an interesting candidate for further experimental investigations.

#### IV. Conclusions

We studied the insertion and elimination steps of the Heck reaction for a model catalyst which contains two strongly coordinating carbene ligands. On the basis of our calculations, we propose a reaction mechanism which proceeds via abstraction of the halide anion and subsequent coordination–insertion of the olefin into the Pd–phenyl bond. This part of the reaction has been calculated for a cationic system in which the halide ion is removed as well as for a neutral system in which the anion stays in the vicinity of the Pd complex. The geometries of the stationary points are not much affected by the presence of the counterion; the calculated barriers to insertion are +8.3 kcal/mol and +11.5 kcal/mol, respectively. The formation of the  $\beta$ -agostic complex **7c** is an endothermic process in contrast to the findings in nonaromatic systems.<sup>19</sup> This difference has been rationalized by the more efficient stabilization of the Pd center by the phenyl ring in the present case compared to the C<sub>β</sub>–H bond. The  $\beta$ -hydride elimination is characterized by a very flat potential energy surface.



The barrier to elimination, 9.0 kcal/mol, is comparable in size to the insertion barrier. The total insertion/elimination process is exothermic by  $-8.9$  kcal/mol.

Furthermore, we have proposed and studied a new type of bidentate ligand which consists of a carbene and a phosphine moiety. This ligand combines the stabilizing effect of the carbene with a labile Pd–P bond which can be broken reversibly to allow for a facile coordination of the olefin to the Pd center. It has been shown that the main features of the insertion are similar to those calculated for the dicarbene system, except for the absence of a second stable  $\pi$  complex formed after

rotation of the ethylene. The barrier to insertion is calculated to be  $+9.2$  kcal/mol, thus being between the corresponding values of the cationic and neutral pathways of the dicarbene system.

**Acknowledgment.** We are indebted to W. A. Herrmann for bringing this subject to their attention, and they thank S. Köstlmeier for a preliminary study on Pd–carbene bonding. This work has been supported by Bayerischer Forschungsverbund Katalyse (FORKAT) and by the Fonds der Chemischen Industrie.

OM9709190